J. Phys. Chem. A **2004,** *108,* 2666−2674

Kinetic Study for the Reactions of Several Hydrofluoroethers with Chlorine Atoms

Vassileios C. Papadimitriou, Kyriakos G. Kambanis, Yannis G. Lazarou,† and Panos Papagiannakopoulos*

Department of Chemistry, University of Crete, Heraklion 71409, Crete, Greece

Received: September 22, 2003; In Final Form: December 31, 2003

The reaction kinetics of chlorine atoms with the hydrofluoroethers $CHF_2CF_2OCH_3$ (1), $CHF_2CF_2OCH_2CH_3$ (2), $CHF_2CF_2OCH_2CF_3$ (3), $CF_3CHFCF_2OCH_3$ (4), and $CH_2{=}CHCH_2OCF_2CHF_2$ (5) were studied in the gas phase over the temperature range 273−363 K. The experiments were performed at very low pressures (<3 mTorr) in a molecular flow system equipped with a quadrupole mass spectrometer by monitoring both reactants. The proposed Arrhenius expressions for the studied reactions are (in cm^3 $molecule^{-1}$ s^{-1}, 2σ uncertainties): $k_1 = (5.49 \pm 1.51) \times 10^{-12} \exp(-928 \pm 155/T)$, $k_2 = (1.99 \pm 0.12) \times 10^{-12} \exp(-36 \pm 33/T)$, $k_3 = (1.95 \pm 0.72) \times 10^{-12} \exp(-1616 \pm 202/T)$, $k_4 = (8.72 \pm 2.93) \times 10^{-12} \exp(-1112 \pm 186/T)$, and $k_5 = (5.54 \pm 1.96) \times 10^{-13} \exp(821 \pm 214/T)$. The title reactions proceed via hydrogen atom metathesis, with the exception of the unsaturated $CH_2{=}CHCH_2OCF_2CHF_2$ ether, where the Cl-atom addition pathway leading to $CH_2{=}CHCl$ is also present. The C−H bond strengths in several hydrofluoroethers were calculated at the B3P86/6-311++G(3df,2p) level of theory, and they show an increase in the order $-OCH(CH_3)-H < -OCH(CF_3)-H < -CH_2OCH_2-H < -CF_2OCH_2-H < -OCH_2CH_2-H < -OCF_2CF_2-H < -OCF_2-H$. Furthermore, their room-temperature rate coefficients correlate with the weakest C−H bond strengths in each molecule, according to the expression log(k, in cm^3 $molecule^{-1}$ s^{-1}) = (23.6 ± 7.4) − (0.09 ± 0.02) × [C−H bond strength (in kJ mol^{-1})]. In addition, their vertical ionization potentials were calculated at the B3LYP/6-311++G(3df,2p) level of theory, and they also correlate with the room-temperature rate coefficients according to the expression log(k, in cm^3 $molecule^{-1}$ s^{-1}) = (4.0 ± 1.7) − (1.42 ± 0.15) × [ionization potential (in eV)].

Introduction

Hydrofluoroethers (HFE) belong to a relatively new generation of chlorine-free compounds harmless to stratospheric ozone, which have been proposed as substitutes for chloroflurocarbons (CFC) and hydrofluorocarbons (HFC), since they contain the ether linkage −O− that is expected to increase their reactivity in the troposphere and reduce their atmospheric lifetimes. Therefore, their impact on global warming and climate changes were anticipated to be negligible.[1−3] The reactivity of a large number of hydrofluoroethers toward atmospheric oxidants and their thermochemical properties have been studied in a number of experimental[3−14] and theoretical[15−19] works. Although the reaction with OH radicals constitutes the main tropospheric sink of hydrofluoroethers, the reaction with the less abundant chlorine atoms may also enhance their removal rates due to the higher reactivity of chlorine atoms toward most organic compounds.[20] In fact, chlorine atoms have been monitored in concentrations in the order of 10^4 molecule cm^{-3} over the marine boundary layer,[21−24] as well as during ozone episodes in urban atmospheres.[25] Furthermore, the reaction kinetics of hydrofluoroethers toward chlorine atoms will provide information on the tropospheric reactivity of hydrofluoroethers, and will also assist in the elucidation of their degradation mechanism in the atmosphere. The kinetic parameters of several hydrofluoroethers with Cl atoms have been determined in a number of studies,[6,7,10,11,26−30] in addition to the study of their tropospheric degradation mechanism[9,11,17] and the reaction kinetics of several hydrofluoroethers with OH radicals,[3−8,12] and O(^{1}D) atoms.[13]

In this work, the absolute rate coefficients for the reactions of chlorine atoms with the hydrofluoroethers $CHF_2CF_2OCH_3$, $CHF_2CF_2OCH_2CH_3$, $CHF_2CF_2OCH_2CF_3$, $CF_3CHFCF_2OCH_3$, and $CH_2{=}CHCH_2OCF_2CHF_2$ were measured over the temperature range 273−363 K. The experiments were performed by using the very low-pressure reactor (VLPR) technique which has been described in detail previously.[31] The reactivity of several hydrofluoroethers as a function of their molecular structure was investigated, by correlating the room-temperature rate coefficients with the C−H bond strengths and the ionization potentials, calculated by the cost-effective density functional theory, with accuracies of ±10 kJ mol^{-1} [32] and ±0.37 eV,[33] respectively.

Experimental Section

The absolute rate coefficients of the title reactions were measured by using a very low pressure reactor (VLPR) apparatus, which has been extensively used in our laboratory for studying the kinetics of fast bimolecular reactions between Cl atoms and a variety of molecules.[10,31,34] The reactor consists of a thermostated cylindrical cell equipped with two capillary inlets for the admission of reactants. The internal surface is coated with a thin film of Teflon (Du-Pont Teflon FEP 120) in order to suppress heterogeneous processes and inhibit Cl atoms recombination. The reaction mixture escapes through an orifice of 5 mm to the first stage of a differentially pumped chamber. An effusive molecular beam is formed by placing a conical skimmer before the second stage of the vacuum chamber. The beam is modulated by a tuning fork chopper with a frequency of 200 Hz, and analyzed by a quadrupole mass spectrometer (Balzers QMG511). A lock-in amplifier is used to discriminate

---

* Corresponding author. E-mail: panosp@chemistry.uoc.gr.

† Present Address: Institute of Physical Chemistry, National Centre for Scientific Research “Demokritos”, Aghia Paraskevi 153 10, Attiki, Greece.

10.1021/jp031081z CCC: $27.50

TABLE 1: Mass Spectra of $CHF_2CF_2OCH_3$, $CHF_2CF_2OCH_2CH_3$, $CHF_2CF_2OCH_2CF_3$, $CF_3CHFCF_2OCH_3$, and $CH_2{=}CHCH_2OCF_2CHF_2$ at an Electron Energy of 19 eV[a]

				$CHF_2CF_2OCH_3$						
m/*e*	15	47	51	81						
	23	5	5	100						
				$CHF_2CF_2OCH_2CH_3$						
m/*e*	15	27	28	29	30	45	79	95	101	131
	38	2	9	100	4.5	5.5	3	8.5	1.5	1.5
				$CHF_2CF_2OCH_2CF_3$						
m/*e*	29	31	33	51	79	83	85	101	131	149
	4.3	70	26.5	12	16.5	100	7	19.5	36	18
				$CF_3CHFCF_2OCH_3$						
m/*e*	15	31	81	82						
	8	3	100	38						
				$CH_2{=}CHCH_2OCF_2CHF_2$						
m/*e*	29	41	51	57	58	59	60	107	158	
	11.5	100	1.5	6	5.5	2	5.5	5	5	

[a] Intensities are reported relative to the intensity of the most prominent mass spectrometric peak.

and amplify the modulated component of the mass spectrometric signal, and a microcomputer is used to collect the output of the lock-in amplifier and control the operation of the mass spectrometer.

The reactants flow into the reactor through a long capillary resistance, and their flow rate (in molecules s^{-1}) is determined by following their buffer volume pressure drop. The escape rate coefficient $k_{esc,M}$ of all species out of the reactor was measured as a function of the molecular weight M, by using their mass spectrometric signal first-order decay after an abrupt halt of their flow. Thus, $k_{esc,M}$ was given by the expression $\beta(T/M)^{1/2}$ (s^{-1}), where the factor β was 2.67 or 1.86, depending on the escape orifice diameter and the reactor volume (for $V_{cell} = 109$ or 168 cm^3, respectively), and *T* was the reactor temperature. The total pressure inside the reactor was estimated to be in the range 0.6−3 mTorr, with a partial pressure of helium of ca. 0.5 mTorr. The residence times of Cl atoms and HFE molecules in the reactor were ca. 0.2 and 0.5 s, respectively.

Chlorine atoms were produced by a microwave discharge in a mixture of 5% Cl_2 in helium flowing through a quartz tube coated with a phosphoric−boric acid mixture. The conversion of Cl_2 molecules to Cl atoms and HCl molecules (produced inside the quartz tube) was almost complete (>97%), and this was verified by monitoring the intensity at *m*/*e* 70 (Cl_2^+). The electron energy in the ion source was set to 19 eV in order to eliminate the contribution of HCl fragmentation to the *m*/*e* 35 (Cl^+) peak, which was measured to be 0.3%. The detection limit of Cl atoms for the current experimental conditions was determined to be ca. 4×10^9 atoms cm^{-3}, based on three times the deviation of the mean background noise.

The mass spectra of all HFEs at an electron energy of 19 eV are shown in Table 1. The steady-state concentration of hydrofluoroethers was determined by monitoring their prominent mass spectrometric peaks, which do not have any contribution from the primary radical product. In particular, $CHF_2CF_2OCH_3$, $CHF_2CF_2OCH_2CH_3$, $CHF_2CF_2OCH_2CF_3$, and $CF_3CHFCF_2OCH_3$ were monitored at their prominent fragment peaks at *m*/*e* 81 ($CH_3OCF_2^+$), *m*/*e* 95 ($CH_3CH_2OCF_2^+$), *m*/*e* 83 ($CF_3CH_2^+$), and *m*/*e* 81 ($CH_3OCF_2^+$), respectively, and $CH_2{=}CHCH_2OCF_2CHF_2$ was monitored at its parent peak at *m*/*e* 158. The relation between the mass spectrometric peak intensity I_S of a given species and its steady-state concentration [S], or flow rate F_S is given by the expression

$$I_S = a_S F_S = a_S V_{cell}\, k_{esc,S}[S]$$

where a_S is a mass spectrometric calibration factor that depends on the selected mass peak.

The rate coefficient measurements were performed by keeping a constant flow rate of chlorine atoms in the reactor, and varying the flow rate of hydrofluoroethers. The initial concentration of chlorine atoms $[Cl]_o$ was on the average 1.5×10^{12} molecule cm^{-3}. At high HFEs flows, the steady-state concentration of HFEs was independent of the Cl atom presence ($[HFE] \cong [HFE]_o$), and the pseudo-first-order approximation for HFEs is valid. In particular for [HFE] > 50[Cl], the rate coefficients could be obtained either by assuming the pseudo-first-order condition for HFEs, or by monitoring the steady-state concentrations of both reactants. The two methods produced identical results within 5%, indicating that the radical products do not interfere with HFEs monitoring. However, the rate coefficients were derived using the second method without relying on the pseudo-first-order assumption.

The steady-state concentrations of Cl atoms and HFE reactants were in the range $(0.1-3) \times 10^{12}$ molecule cm^{-3} and $(0.001-3.5) \times 10^{14}$ molecule cm^{-3}, respectively. The uncertainty in the mass spectral intensity measurements was ca. 5% (2σ), leading to an accuracy of ca. 7% (2σ) for the ratio $R = [Cl]_o/[Cl] = I_{Cl_o}/I_{Cl}$.

The title hydrofluoroethers were commercially available and their source and stated purity were the following: $CHF_2CF_2OCH_3$ (Fluorochem, 98%); $CHF_2CF_2OCH_2CH_3$, $CHF_2CF_2OCH_2CF_3$, and $CF_3CHFCF_2OCH_3$ (Fluorochem, 97%); $CH_2{=}CHCH_2OCF_2CHF_2$ (Aldrich, 99%). However, they were further purified by fractional distillation and degassing at 77 K, achieving 99% purity, as indicated by GC/MS and NMR analysis.

Results

Mass spectrometric analysis of the products for the title reactions revealed the appearance of HCl (at *m*/*e* 36) as the primary reaction product. In addition, for the reaction of the unsaturated ether (5), vinyl chloride ($CH_2{=}CHCl$ at *m*/*e* 62 and 64) was detected among the reaction products, indicating the presence of the chlorine atom addition pathway.

Thus, all reactions proceed via a hydrogen transfer mechanism as shown below:

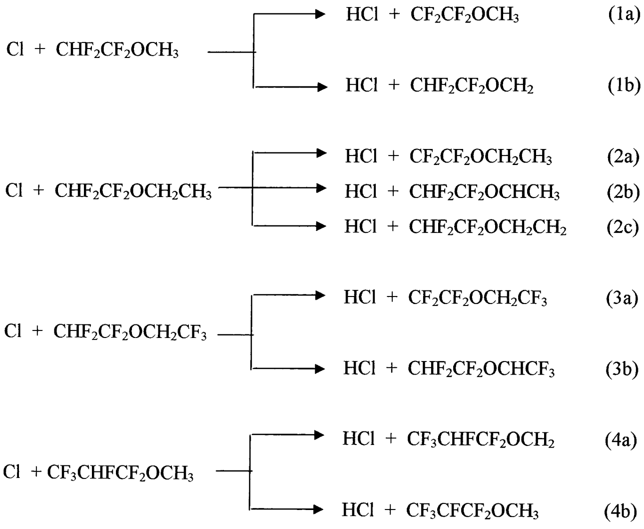

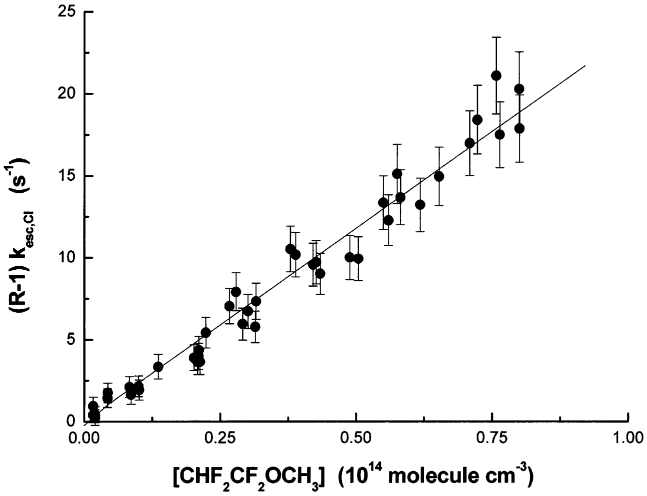

Figure 1. Plot of ($R - 1$) $k_{esc,Cl}$ vs [$CHF_2CF_2OCH_3$] at $T = 303$ K. Error bars reflect the propagated error (2σ), solid line is the linear least-squares fit to the data.

In particular, the reaction of $CH_2{=}CHCH_2OCF_2CHF_2$ proceeds via the following pathways:

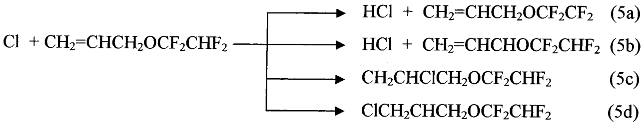

The intermediate adducts in reactions 5c and 5d may further undergo unimolecular decomposition via C−C or C−O bond fission, yielding the corresponding chloroalkenes:

$$CH_2CHClCH_2OCF_2CHF_2 \rightarrow CH_2{=}CHCl + CH_2OCF_2CHF_2 \quad (5e)$$

$$ClCH_2CHCH_2OCF_2CHF_2 \rightarrow ClCH_2CH{=}CH_2 + OCF_2CHF_2 \quad (5f)$$

All experiments were performed at very low pressures (0.6−3 mTorr range) in order to suppress any secondary reactions. The recombination and abstraction reactions between Cl atoms and primary radicals leading to chlorinated products, as well as the radical−radical reactions, could not occur at low-pressure conditions. Indeed, our experiments have verified the absence of any chlorinated products, with the exception of reaction 5, where the Cl atom addition pathway is present. Therefore, secondary reactions of Cl atoms were not included in the above reaction schemes, and application of the steady-state approximation for each reaction leads to the expression

$$\Delta[\mathrm{Cl}]k_{esc,Cl} = k[\mathrm{Cl}][\mathrm{HFE}]$$

where Δ[Cl] is the difference of the steady-state concentrations, $[\mathrm{Cl}]_o - [\mathrm{Cl}]_r$ (subscripts o and r denote the absence or presence of HFE reactant, respectively), $k_{esc,Cl}$ is the escape rate of Cl atoms, k is the rate coefficient (the sum of all primary reaction pathways), and [HFE] is the steady-state concentration of the HFE. The rearrangement of the above expression leads to

$$(R - 1)k_{esc,Cl} = k[\mathrm{HFE}]$$

where $R = [\mathrm{Cl}]_o/[\mathrm{Cl}]_r = I_{35,o}/I_{35,r}$. Therefore, all experiments were performed by monitoring the mass spectral signals of both reactants while a given flow of HFE was introduced into the reactor. A typical plot of the above expression for the reaction with ether (1) at $T = 303$ K is presented in Figure 1. The linear least-squares fits to the data yield the rate coefficients with a precision of ca. 10% (2σ).

Experiments were performed at temperatures of 273, 303, 333, and 363 K, and the rate coefficient values obtained at each temperature are listed in Table 2. Linear least-squares fits of the temperature-dependent rates yield the activation energies and the preexponential Arrhenius factors, which are given in Table 3. Finally, the Arrhenius plots of all title reactions are presented in Figure 2.

Theoretical Calculations of the C−H Bond Strengths and the Ionization Potentials of Hydrofluoroethers

The electronic structure calculations were performed with the Gaussian 98 programs suite.[35] Spin-restricted wave functions were selected for all closed-shell molecules, while unrestricted ones were selected for the radicals. The geometries and the vibrational frequencies of all species were calculated by using the B3P86 density theory functional[36,37] in combination with the small 6-31G(d′) basis set,[38] which employs more realistic values for the d polarization function exponents for the first-row atoms than the commonly used 6-31G(d).[39] All vibrational frequencies were scaled by 0.9723 to compensate for the deficiencies of the B3P86/6-31G(d′) level of theory.[32] Subsequently, single-point calculations were performed by employing

TABLE 2: Rate Coefficients Measured for the Title Reactions (in 10^{-15} cm^3 $molecule^{-1}$ s^{-1}, 2σ uncertainty) at the Temperatures 273, 303, 333, and 363 K[a]

	temperature					
HFE	273	303	333	363	$[\mathrm{HFE}]_o$ range	$(R - 1)k_{esc,Cl}$ range
$CHF_2CF_2OCH_3$	185 ± 20	236 ± 49	344 ± 28	421 ± 52	$0.2{-}9.0 \times 10^{13}$	0.4−30
$CHF_2CF_2OCH_2CH_3$	1750 ± 220	1750 ± 210	1800 ± 220	1800 ± 150	$0.2{-}4.0 \times 10^{13}$	4−50
$CHF_2CF_2OCH_2CF_3$	5.28 ± 0.52	9.11 ± 1.03	16.3 ± 2.3	22.2 ± 3.0	$0.3{-}3.5 \times 10^{14}$	0.3−5
$CF_3CHFCF_2OCH_3$	146 ± 18	231 ± 41	323 ± 52	391 ± 62	$0.3{-}2.5 \times 10^{13}$	0.2−7
$CH_2{=}CHCH_2OCF_2CHF_2$	11100 ± 1300	8320 ± 680	6760 ± 830	4950 ± 990	$0.3{-}6.8 \times 10^{12}$	2−60

[a] The ranges of $[\mathrm{HFE}]_o$ and (R-1)$k_{esc,Cl}$ for each reaction and at all temperatures are also listed. HFE concentrations are in molecule cm^{-3}.

TABLE 3: Kinetic Parameters and Rate Coefficients at 298 K (interpolated by the corresponding Arrhenius expressions) for the Reactions of Cl Atoms with the Hydrofluoroethers of the Present Study

HFE	A cm^3 $molecule^{-1}$ s^{-1}	E_a/R K	k_{298} cm^3 $molecule^{-1}$ s^{-1}
$CHF_2CF_2OCH_3$	$(5.49 \pm 1.51) \times 10^{-12}$	928 ± 155	$(2.44 \pm 1.44) \times 10^{-13}$
$CHF_2CF_2OCH_2CH_3$	$(1.99 \pm 0.12) \times 10^{-12}$	36 ± 33	$(1.76 \pm 0.22) \times 10^{-13}$
$CHF_2CF_2OCH_2CF_3$	$(1.95 \pm 0.72) \times 10^{-12}$	1616 ± 202	$(8.63 \pm 6.66) \times 10^{-15}$
$CF_3CHFCF_2OCH_3$	$(8.72 \pm 2.93) \times 10^{-12}$	1112 ± 186	$(2.09 \pm 1.48) \times 10^{-13}$
$CH_2{=}CHCH_2OCF_2CHF_2$	$(5.54 \pm 1.96) \times 10^{-13}$	−821 ± 214	$(8.70 \pm 6.96) \times 10^{-12}$

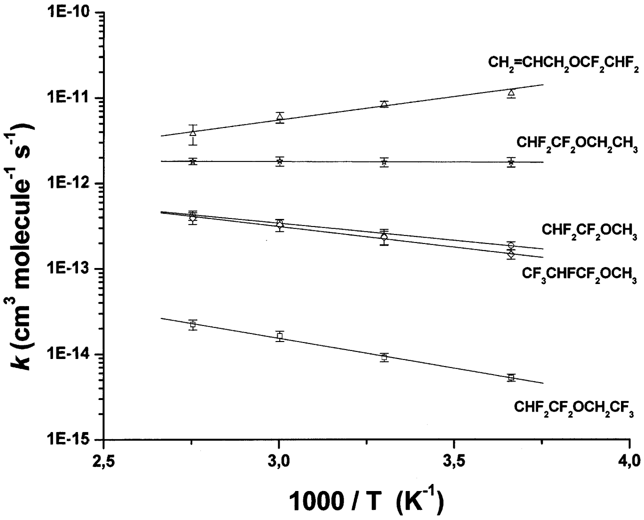

Figure 2. Arrhenius plots for the title reactions. Error bars reflect the propagated errors (2σ), solid lines are the linear least-squares fits to the data.

the B3P86 functional and the extended 6-311++G(3df,2p) basis set.[40] It is known that the B3P86 functional in combination with medium to large basis sets is a rather accurate method for calculating molecular geometries and bond strengths for halogenated species.[32] Finally, zero-point energies and thermal corrections at 298.15 K were added to the high-level electronic energies by assuming the rigid rotor and harmonic oscillator approximations in order to obtain the total enthalpies and the bond dissociation energies at 298.15 K.

The C−H bond strengths for most hydrofluoroethers available in the literature were calculated at B3P86/6-31G(d′) and B3P86/6-311++G(3df,2p) and are presented in Table 4. It is interesting to note that both levels of theory yield comparable values of C−H bond strengths within 8 kJ mol^{-1}. The only experimentally known value of C−H bond strength is for CH_3OCH_3, 393.7 ± 10.0 kJ mol^{-1} (calculated from the corresponding formation enthalpies of CH_3OCH_3, −184.1 ± 0.50 kJ mol^{-1} [41], CH_3OCH_2, −8.4 ± 10 kJ mol^{-1},[42] and H, 217.998 ± 0.006 kJ mol^{-1} [43]) which is close to the 401.9 kJ mol^{-1} value, derived at the highest level of theory. In addition, the C−H bond strengths were calculated for several fluorinated dimethyl ethers and the values obtained were similar to those in previous calculations at the MP2/6-311++G(2d,2p) level of theory.[18] Finally, the reaction enthalpy at 298.15 K for all possible pathways for the reaction of Cl atom with $CH_2{=}CHCH_2OCF_2CHF_2$ were also calculated and are presented in Table 5.

The vertical ionization potentials of most hydrofluoroethers available in the literature were calculated at the B3LYP/6-311++G(3df,2p) level of theory by taking the difference between the absolute electronic energies of the title ether and the corresponding singly ionized cation (retaining the parent molecule geometry), and these values are listed in Table 6. It has been recently shown that the B3LYP functional yields accurate ionization potentials for several molecules containing first-row atoms.[33] Indeed, the calculated ionization potentials, presented in Table 6, indicate an excellent agreement with the corresponding experimental values for CH_3OCH_3,[44] $CH_3CH_2OCH_3$,[45] $CF_3CH_2OCH_3$,[46] and $CH_3CH_2OCH_2CH_3$.[45]

TABLE 4: C−H Bond Strengths (in kJ mol^{-1}) at 298.15 K of Hydrofluoroethers at the B3P86/6-31G(d′) and B3P86/6-311++G(3df,2p) Levels of Theory

bond	B3P86/ 6-31G(d′)	B3P86/ 6-311++G(3df,2p)	bond	B3P86/ 6-31G(d′)	B3P86/ 6-311++G(3df,2p)
CH_3OCH_2-H	409.1	401.9	$CF_3CF_2OCH_2-H$	426.7	422.7
CH_2FOCH_2-H	399.9	395.5	cyclo-($OCF_2CF(-H)CF_2$)	430.4	431.9
$CH_3OCHF-H$	394.6	394.7			
			$CH_3CH_2OCH(-H)CH_3$	398.7	392.1
CHF_2OCH_2-H	421.1	415.7	$CH_3CH_2OCH_2CH_2-H$	435.4	428.1
CH_3OCF_2-H	423.3	422.5			
			$CHF_2CF_2OCH_2CH_2-H$	437.2	431.3
CF_3OCH_2-H	426.0	421.6	$CHF_2CF_2OCH(-H)CH_3$	412.1	407.8
			$CH_3CH_2OCF_2CF_2-H$	424.5	425.8
$CH_2FOCHF-H$	419.3	418.5			
			$CF_3CH_2OCH(-H)CF_3$	408.9	401.0
$CHF_2OCHF-H$	423.7	420.4			
CH_2FOCF_2-H	437.9	439.2	$CHF_2CF_2OCH(-H)CF_3$	418.6	415.2
			$CF_3CH_2OCF_2CF_2-H$	425.2	427.2
$CF_3OCHF-H$	423.5	421.0			
			$CF_3CHFCF_2OCH_2-H$	425.6	420.5
CHF_2OCF_2-H	434.9	435.0	$CH_3OCF_2CF(-H)CF_3$	419.1	415.2
CF_3OCF_2-H	430.0	424.3	$CHF_2CF_2CH_2OCF_2-H$	426.0	423.2
			$CHF_2CF_2CH(-H)OCHF_2$	413.8	399.5
$CH_3CH_2OCH_2$-H	408.6	401.6	$CHF_2OCH_2CF_2CF_2-H$	423.4	418.9
$CH_3CH(-H)OCH_3$	399.0	392.2			
$CH_3OCH_2CH_2$-H	435.6	428.3	$(CF_3)_2CHOCF_2-H$	425.6	424.7
			$(CF_3)_2C(-H)OCHF_2$	407.8	410.0
$CF_3CH_2OCH_2-H$	413.0	406.4			
$CF_3CH(-H)OCH_3$	399.7	392.2	n-$C_3F_7OCH_2-H$	422.5	416.7
$CHF_2CF_2OCH_2-H$	425.4	420.8	i-$C_3F_7OCH_2-H$	420.2	415.3
$CH_3OCF_2CF_2-H$	424.0	425.8			
			n-$C_4F_9OCH_2-H$	427.4	423.3
$CF_3CH_2OCF_2-H$	440.9	440.9			
$CF_3CH(-H)OCHF_2$	421.5	416.8	n-$C_4F_9OCH_2CH_2-H$	437.2	432.6
			n-$C_4F_9OCH(-H)CH_3$	411.9	406.3
$CH_2FCF_2OCF_2$-H	432.5	429.1			
CHF_2OCF_2CHF-H	423.6	419.6	$CH_2{=}CHCH_2OCF_2CF_2-H$	424.5	426.3
			$CH_2{=}CHCH-H)OCF_2CHF_2$	345.8	343.1

TABLE 5: Theoretical Reaction Enthalpies (in kJ mol^{-1}) at 298.15 K for the Most Probable Reactions of the System $CH_2{=}CHCH_2OCF_2CHF_2$ + Cl, at the B3P86/6-311++G(3df,2p) Level of Theory

reaction	B3P86/ 6-311++G(3df,2p)
$CH_2{=}CHCH_2OCF_2CHF_2 + Cl \rightarrow ClCH_2CHCH_2OCF_2CHF_2$	−105.7
$CH_2{=}CHCH_2OCF_2CHF_2 + Cl \rightarrow CH_2CHClCH_2OCF_2CHF_2$	−97.2
$ClCH_2CHCH_2OCF_2CHF_2 \rightarrow CH_2CHClCH_2OCF_2CHF_2$	8.5
$ClCH_2CHCH_2OCF_2CHF_2 \rightarrow ClCH_2CH{=}CH_2 + CHF_2CF_2O$	120.5
$CH_2CHClCH_2OCF_2CHF_2 \rightarrow CH_2{=}CHCl + CHF_2CF_2OCH_2$	99.9
$CH_2CHClCH_2OCF_2CHF_2 \rightarrow CH_2{=}CHCHOCF_2CHF_2 + HCl$	−4.1
$CH_2CHClCH_2OCF_2CHF_2 \rightarrow CH_2{=}CHCH_2OCF_2CF_2 + HCl$	79.1
$ClCH_2CHCH_2OCF_2CHF_2 \rightarrow CH_2{=}CHCHOCF_2CHF_2 + HCl$	4.4
$ClCH_2CHCH_2OCF_2CHF_2 \rightarrow CH_2{=}CHCH_2OCF_2CF_2 + HCl$	87.6
$CH_2{=}CHCH_2OCF_2CHF_2 + Cl \rightarrow CH_2{=}CHCl + CHF_2CF_2OCH_2$	2.7
$CH_2{=}CHCH_2OCF_2CHF_2 + Cl \rightarrow ClCH_2CH{=}CH_2 + CHF_2CF_2O$	14.8
$CH_2{=}CHCH_2OCF_2CHF_2 + Cl \rightarrow CH_2{=}CHCHOCF_2CHF_2 + HCl$	−101.3
$CH_2{=}CHCH_2OCF_2CHF_2 + Cl \rightarrow CH_2{=}CHCH_2OCF_2CF_2 + HCl$	−18.1

TABLE 6: Vertical Ionization Potentials (in eV) of Several Hydrofluoroethers Calculated at the B3LYP/6-311++G(3df,2p) Level of Theory[a]

ether	ionization potential (eV) B3LYP/6-311++G(3df,2p)
CH_3OCH_3	9.99 (10.025 ± 0.25, ref 44)
CH_2FOCH_3	10.48
CHF_2OCH_3	11.49
CF_3OCH_3	12.07
CH_2FOCH_2F	11.96
CHF_2OCH_2F	12.50
CF_3OCH_2F	13.12
CHF_2OCHF_2	12.79
CF_3OCHF_2	13.45
$CH_3CH_2OCH_3$	9.77 (9.72 ± 0.07, ref 45)
$CF_3CH_2OCH_3$	10.63 (10.53, ref 46)
$CHF_2CF_2OCH_3$	11.76
$CF_3CH_2OCHF_2$	12.13
$CF_3CF_2OCH_3$	12.06
$CH_2FCF_2OCHF_2$	12.61
cyclo-OCF_2CHFCF_2	12.89
$CH_3CH_2OCH_2CH_3$	9.59 (9.52 ± 0.07, ref 45)
$CHF_2CF_2OCH_2CH_3$	11.39
$CF_3CH_2OCH_2CF_3$	11.06
$CHF_2CF_2OCH_2CF_3$	12.13
$CF_3CHFCF_2OCH_3$	11.80
$CHF_2CF_2CH_2OCHF_2$	11.26
i-$C_3F_7OCH_3$	11.23
n-$C_3F_7OCH_3$	11.49
$(CF_3)_2CHOCHF_2$	12.20
n-$C_4F_9OCH_3$	11.72
n-$C_4F_9OCH_2CH_3$	11.42
$CF_2{=}CFOCF_3$	10.43
$CH_2{=}CHCH_2OCF_2CHF_2$	10.29

[a] Experimental values are shown in parentheses.

Discussion

The Arrhenius parameters and the rate coefficients at 303 K for the title reactions are presented in Table 3. The room-temperature rate coefficients for hydrogen atom metathesis reactions span the range from 9.11×10^{-15} for $CHF_2CF_2OCH_2CF_3$ to 1.75×10^{-12} cm^3 molecule^{-1} s^{-1} for $CHF_2CF_2OCH_2CH_3$, and reach the highest value of 8.32×10^{-12} cm^3 molecule^{-1} s^{-1} for the unsaturated $CH_2{=}CHCH_2OCF_2CHF_2$ ether, where the Cl-addition pathway competes with the H-atom abstraction pathway. The variation of the rate coefficients for the hydrogen atom metathesis reactions can be explained either in terms of reaction enthalpies[47] that reflect the variations in the C−H bond strengths, or in terms of ionic curve-crossing states of the species involved which correlate strongly with the ionization potentials[48,49] or the energies of the HOMO[50] of HFEs. These molecular properties can be determined either experimentally or predicted by electronic structure calculations, and can be employed in the construction of empirical structure−reactivity relationships.[51−55]

It has been argued that the correlation between the rate coefficients and the properties affecting the ionic states of the species involved (ionization potentials, electron affinities) is more accurate than the correlation with the thermochemical properties, in particular the barrier heights.[48,49] However, for the reactions of electrophilic radicals (Cl, OH) with a particular class of compounds, the key molecular properties are all strongly interrelated, leading to structure−reactivity relationships of comparable quality by either approach. In addition, the thermochemical approach is advantageous regarding its ability to suggest the most likely sites of atom metathesis, by taking into account the relative strengths of the various C−H bonds in a molecule, besides entropic factors.

Experimental data indicate that for most saturated organic molecules, the presence of the ether linkage −O− increases the molecular reactivity by significantly lowering the activation energy of hydrogen atom metathesis reactions.[20,56] However, theoretical calculations have suggested that the presence of adjacent fluorine atoms suppresses or even reverses the deactivating effect of the ether link, as in the case of $-OCHF_2$ group.[18,19] In addition, experimental[56−62] and theoretical[18,19,32,63] studies have shown that substitution by a single halogen atom lowers the C−H bond strengths and enhances the abstraction of adjacent hydrogen atoms, while it strengthens the C−H bonds on the vicinal carbon atoms. The effects of halogen substitution on the rate coefficient have been also discussed in terms of the charge distribution affecting the energetics of the transition state by the approach of the electrophilic Cl atom.[61]

In general, the strength of the C−H bonds in hydrofluoroethers depends on the interplay of two counteracting electronic effects: (a) the strengthening due to the electron-withdrawing inductive effects of F and/or O atoms through σ-bonds, and (b) the weakening of the adjacent C−H bonds due to the π-electron transfer from F or O atom to the central C atom. This general qualitative scheme, in terms of electronic interactions, may provide an adequate explanation for the observed trend of C−H bond strengths shown in Table 4. In principle, fluoroethers may be divided in seven types and furthermore in two main groups, considering their structure and the strength of the C−H bond, and in accordance with the bond strength: (a) $-OCH_2CH_2-H$, $-OCF_2CF_2-H$, and (b) $-OCF_2-H$, $-CF_2OCH_2-H$, $-CH_2$-

OCH_2−H, −$OCH(CF_3)$−H, and −$OCH(CH_3)$-H. In the first group, C−H bond strengths are of similar magnitude (429.2 ± 3.4 kJ mol^{-1}) and very strong since they cannot be affected by the conjugative effects of the O atom. In the second group, C−H bonds are adjacent to O atoms, therefore they are affected by conjugative effects, thus the bond strengths are weaker than in the first group, with the exception of the −OCF_2−H bond that is the strongest (ca. 435 kJ mol^{-1}) due to the inductive effects of the adjacent O and F atoms. The −CF_2OCH_2−H bonds are sufficiently strong (ca. 420 kJ mol^{-1}) due probably to the inductive effects of the R_FCF_2O− group (R_F = H, F, CHF_2, CF_3, CF_3CHF, CF_3CF_2, $CF_3CF_2CF_2$). The last three types of C−H bonds represent the weakest members of the series with bond strengths in the range 392−417 kJ mol^{-1}. The strongest bonds for each type are $CF_3CH_2OCH_2$−H (406.4 kJ mol^{-1}), $CHF_2OCH(CF_3)$−H (416.8 kJ mol^{-1}), and $CHF_2CF_2OCH(CH_3)$−H (407.8 kJ mol^{-1}), as a result of the inductive effects of the corresponding fluorinated groups connected to the oxygen atom.

The mass spectrometric analysis of the reaction products suggests that the reaction of Cl atoms with $CH_2{=}CHCH_2OCF_2CHF_2$ occurs via hydrogen atom transfer as well as via Cl atom addition pathway. The presence of the addition pathway is also indicated by the negative activation energy, $E_a = -6.8 \pm 1.8$ kJ mol^{-1}. The standard enthalpy for all probable pathways were calculated at the B3P86/6-311++G(3df,2p) level of theory, and is presented in Table 5. The Cl atom addition to the terminal C atom is thermochemically more favorable by 8.5 kJ mol^{-1}, which is probably due to hyperconjugative interactions between the −CH_2Cl and −CH_2− groups and the singly occupied carbon p-orbital in the $ClCH_2CHCH_2OCF_2CHF_2$ adduct. The addition pathways leading to $CH_2{=}CHCl$ and $CH_2{=}CHCH_2Cl$ are mildly endothermic by 2.7 and 14.7 kJ mol^{-1}, respectively; therefore the $CH_2{=}CHCl$ formation pathway is thermodynamically more favorable and in agreement with experimental results. The production of HCl versus the consumption of Cl (Δ[HCl]/Δ[Cl]) was found to increase with temperature from 0.66 ± 0.15 at 273 K to 0.81 ± 0.21 at 363 K, leading to a branching ratio $[CH_2{=}CHCl]/[HCl]$ varying from 0.52 at 273 K to 0.23 at 363 K. Experimental data indicate that HCl formation is the predominant pathway at low pressures and the particular range of temperatures. Moreover, the magnitude of the negative activation energy and the relatively high rate coefficient suggest that the overall reaction proceeds mainly through an intermediate complex. The high exothermicity (ca. 100 kJ mol^{-1}) for the complex formation process suggests that long-range attractive interactions between Cl atoms and $CH_2{=}CHCH_2OCF_2CHF_2$ molecules favor a hot complex formation, rather than a direct H atom abstraction. The enthalpy for the HCl elimination pathway yielding the $CH_2{=}CHCHOCF_2CHF_2$ radical is ca. 100 kJ mol^{-1} lower than the entropically more favorable C−C bond fission pathway yielding $CH_2{=}CHCl$. This may explain the preference for HCl formation that occurs mainly via the decomposition of the intermediate complex.

It is interesting to study the correlation between the rate coefficients and the C−H bond strengths for hydrofluoroethers. However, for molecules possessing more than one site of H abstraction it is reasonable to assume that the weakest C−H bond will have the highest contribution to the overall rate, while the preexponential factors are within a small range of values. Furthermore, for similar abstraction reactions of Cl atoms, it is expected that the activation energy will be a linear function of the weakest C−H bond strength. A plot of log(*k*) for known room-temperature rate coefficients (excluding $CH_2{=}CHCH_2OCF_2CHF_2$) as a function of the lowest C−H bond strengths (calculated at B3P86/6-311++G(3df,2p) level of theory) is shown in Figure 3. The linear least-squares fit yields the expression log(*k*, in cm^3 $molecule^{-1}$ s^{-1}) = (23.6 ± 7.4) − (0.09 ± 0.02) × [BDE_{C-H} (kJ mol^{-1})]. For several ethers, and in particular for $CHF_2CF_2OCH_2CF_3$, CH_3OCH_3, $CF_3CH_2OCHF_2$, CHF_2OCHF_2, and $CH_3CH_2OCH_2CH_3$, the rate coefficients calculated by this empirical expression deviate more than an order of magnitude from the experimental values. These deviations may be due to inaccuracies of experimental and theoretical data as well as to the neglect of entropy, which is largely associated with preexponential factors and affects the branching ratios for molecules with various reactive sites. Therefore, for the reactions of Cl atoms with HFEs, it is possible to have an approximate estimation of the room-temperature rate coefficients by using C−H bond strengths calculated at the computationally affordable B3P86/6-311++G(3df,2p) level of theory.

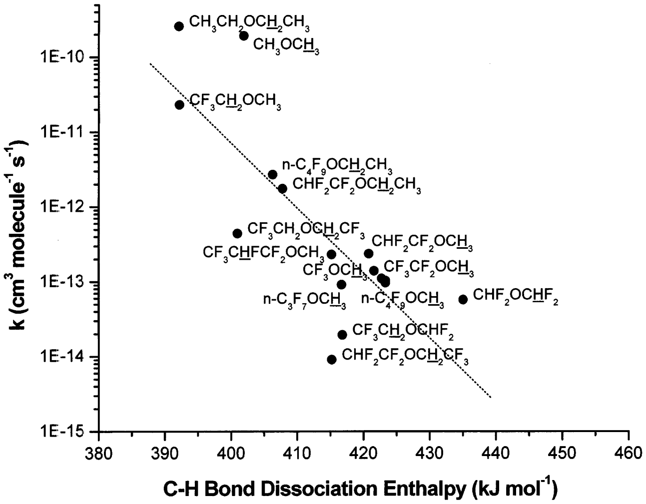

Figure 3. Plot of all known experimental rate coefficients at room temperature for Cl atoms with hydrofluoroethers versus the strength of their weakest C−H bonds (with the corresponding H atom underlined), calculated at the B3P86/6-311++G(3df,2p) level of theory.

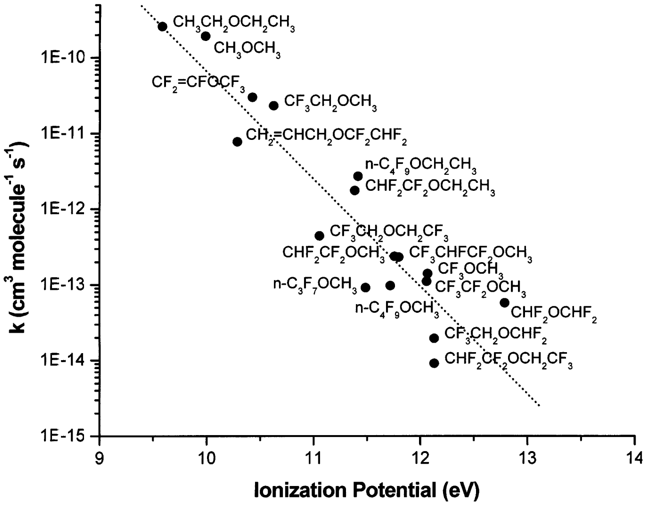

Figure 4. Plot of all known experimental rate coefficients at room temperature for Cl atoms with hydrofluoroethers versus their vertical ionization potentials calculated at the B3LYP/6-311++G(3df,2p) level of theory.

Similarly, the correlation between room-temperature rate coefficients of Cl atom reactions with HFEs (including the unsaturated $CH_2{=}CHCH_2OCF_2CHF_2$ and $CF_2{=}CFOCF_3$ ethers) and properties associated with molecular ionic states was also examined by plotting log(*k*) versus the calculated vertical ionization potentials (IP) of HFEs at the B3LYP/6-311++G(3df,2p) level of theory, as shown in Figure 4. A linear least-

TABLE 7: Room Temperature Rate Coefficients of Hydrofluoroethers with OH Radicals and Cl Atoms

HFEs	k_{OH}	ref	k_{Cl}	ref
CF_3OCH_3	2.14×10^{-14}	1	1.4×10^{-13}	11
	1.0×10^{-14}	3		
	1.20×10^{-14}	65		
CHF_2OCHF_2	2.53×10^{-14}	1	5.73×10^{-14}	10
	2.3×10^{-15}	3		
	2.47×10^{-15}	12		
CF_3OCHF_2	3.38×10^{-15}	1		
	4.2×10^{-16}	3		
$CF_3CH_2OCH_3$	6.24×10^{-13}	1	2.31×10^{-11}	10
$CHF_2CF_2OCH_3$	2.04×10^{-13}	66	2.36×10^{-13}	This work
	2.24×10^{-14}	67		
$CF_3CH_2OCHF_2$	1.25×10^{-14}	1	3.11×10^{-14}	10
			1.20×10^{-14}	26
			1.2×10^{-14}	27
$CF_3CF_2OCH_3$	1.10×10^{-14}	68	1.1×10^{-13}	28
$CH_2FCF_2OCHF_2$	5.50×10^{-15}	69		
$CHF_2CF_2OCH_2CH_3$	4.33×10^{-13}	66	1.75×10^{-12}	This work
	2.24×10^{-13}	70		
$CHF_2CF_2OCH_2CF_3$	9.35×10^{-14}	66	9.11×10^{-15}	This work
	9.16×10^{-15}	67		
	9.5×10^{-15}	69		
$CF_3CH_2OCH_2CF_3$	1.63×10^{-13}	12	4.40×10^{-13}	10
			7.1×10^{-13}	9
$CF_3CHFCF_2OCH_3$	1.05×10^{-14}	67	2.31×10^{-13}	This work
$CF_3CF_2CF_2OCH_3$	1.06×10^{-14}	68	9.1×10^{-14}	29
			1.18×10^{-13}	28
$(CF_3)_2CFOCH_3$	1.45×10^{-14}	68		
$(CF_3)_2CHOCHF_2$	7.5×10^{-14}	71		
$CHF_2CF_2CH_2OCHF_2$	1.62×10^{-14}	69		
$CF_3CHFCF_2OCH_2CF_3$	8.9×10^{-15}	69		
$CF_3CF_2CF_2CF_2OCH_3$	1.2×10^{-14}	6	9.7×10^{-14}	6
$CF_3CHFCF_2OCH_2CF_2CHF_2$	1.20×10^{-14}	69		
$CF_3CF_2CF_2CF_2OCH_2CH_3$	6.4×10^{-14}	7	2.7×10^{-12}	7
$(CF_3)_2CFCF_2OCH_2CH_3$	7.7×10^{-14}	7	2.7×10^{-12}	7
$CF_3CF_2CF_2CF_2CF_2OCH_3$			1.03×10^{-13}	28
cyclo-(CF_2CHFCF_2O)	2.51×10^{-15}	1		
cyclo-$(CF_2CF_2CF_2O)$	$<2 \times 10^{-16}$	1		
$CF_3OCF{=}CF_2$	2.96×10^{-12}	72	3.0×10^{-11}	30
	2.6×10^{-12}	30		
$CH_2{=}CHCH_2OCF_2CHF_2$	1.85×10^{-11}	66	8.32×10^{-12}	This work
$CHFClCF_2OCH_3$	1.65×10^{-13}	66		
	3.76×10^{-14}	70		
$CHFClCF_2OCHF_2$	1.6×10^{-14}	71	4.3×10^{-15}	26
$CF_3CHClOCHF_2$	2.1×10^{-14}	71	4.3×10^{-15}	26
			5.4×10^{-15}	27
$CF_3CH_2OCClF_2$			2.85×10^{-15}	26

squares fit yields the expression log(k, in cm^3 $molecule^{-1}$ s^{-1}) = $(4.0 \pm 1.7) - (1.42 \pm 0.15) \times$ [IP(eV)].

The room temperature rate coefficients with OH radicals and Cl atoms for all hydrofluoroethers available in the literature are shown in Table 7, to allow the comparison of their reactivity with these significant tropospheric species. In general, the Cl atoms react faster than OH radicals with HFEs, with the exception of the heavily halogen-substituted ethers $CHF_2CF_2OCH_2CF_3$, $CHFClCF_2OCHF_2$, $CF_3CHClOCHF_2$ and the unsaturated $CH_2{=}CHCH_2OCF_2CHF_2$ ether, and the ratio k_{Cl}/k_{OH} is decreasing as the C−H bonds become stronger, as observed for most halogenated hydrocarbons.[20]

TABLE 8: Room Temperature Rate Coefficients of Most Common HFCs and Various HFEs with OH Radicals and Cl Atoms (in 10^{-15} cm^3 $molecule^{-1}$ s^{-1}), and the Corresponding Tropospheric Lifetimes t (in years)

	k_{OH}[a]	k_{Cl}[a]	τ_{OH}[b]	τ_{Cl}[b]	τ_{eff}[b]
CH_2F_2	10	50	3.2	63	3.0
CHF_3	0.3	0.003	106	1.1×10^6	105
CHF_2CH_3	35	260	0.9	12	0.8
CF_3CH_3	1.2	0.03	26	1.1×10^5	26
CF_3CH_2F	4.2	1.5	7.5	2112	7.5
CF_3CHF_2	1.9	0.2	17	1.6×10^4	17
$CF_3CH_2CHF_2$	7.0	6.9[c]	4.5	459	4.5
$CF_3CH_2CF_3$	0.3	0.01[d]	106	3.2×10^5	106
CF_3CHFCF_3	1.7	0.04[e]	19	7.9×10^4	19
$CF_3CH_2CF_2CH_3$	5.7	1.1[d]	5.6	2880	5.5
$CF_3CHFCHFCF_2CF_3$	3.4	-	9.3	-	9.3
CF_3OCH_3	12[f]	140[q]	2.6	23	2.4
CHF_2OCHF_2	2.5[g]	57[r]	13	56	10
$CF_3CH_2OCH_3$	624[h]	2310[r]	0.1	1.4	0.05
$CHF_2CF_2OCH_3$	22[i]	236[s]	1.4	13	1.3
$CF_3CH_2OCHF_2$	12[h]	31[r]	2.6	102	2.6
$CF_3CF_2OCH_3$	11[j]	110[t]	2.9	29	2.6
$CHF_2CF_2OCH_2CH_3$	224[k]	1750[s]	0.1	1.8	0.1
$CHF_2CF_2OCH_2CF_3$	9.5[l]	9.1[s]	3.3	348	3.3
$CF_3CH_2OCH_2CF_3$	163[g]	440[r]	0.2	7.2	0.2
$CF_3CHFCF_2OCH_3$	10[i]	231[s]	3.2	14	2.6
$CF_3CF_2CF_2OCH_3$	10[j]	118[t]	3.2	27	2.8
$CF_3CF_2CF_2CF_2OCH_3$	12[m]	97[m]	2.6	33	2.4
$CF_3CF_2CF_2CF_2OCH_2CH_3$	64[n]	2700[n]	0.5	1.2	0.3
$CF_3OCF{=}CF_2$	2600[o]	30000[o]	0.01	0.1	0.01
$CH_2{=}CHCH_2OCF_2CHF_2$	18500[p]	8320[s]	0.002	0.4	0.002

[a] Rate coefficients for the reactions of most HFCs with OH and Cl taken from ref 20. [b] τ_{OH}, τ_{Cl} are based on diurnal average concentrations [OH] and [Cl] of 1×10^6,[64] and 1×10^4 molecule cm^{-3},[23] respectively, and τ_{eff} represents the effective lifetime, according to the expression $1/\tau_{eff} = 1/\tau_{OH} + 1/\tau_{Cl}$. [c] Ref 73. [d] Ref 74. [e] Ref 75. [f] Ref 65. [g] Ref 12. [h] Ref 1. [i] Ref 67. [j] Ref 68. [k] Ref 70. [l] Ref 69. [m] Ref 6. [n] Ref 7. [o] Ref 30. [p] Ref 66. [q] Ref 11. [r] Ref 10. [s] This work. [t] Ref 28.

The reactivity of hydrofluoroethers toward OH radicals and Cl atoms has been measured to be higher than those of most commonly used hydrofluorocarbons, and the pertinent data are presented in Table 8. Their tropospheric lifetimes t_{eff} were calculated by assuming that their removal from the atmosphere occurs only via chemical reactions with OH and Cl, with lifetimes t_{OH} and t_{Cl}, respectively:

$$1/t_{eff} = 1/t_{OH} + 1/t_{Cl}$$

where $t_{OH} = 1/k_{OH}[OH]$ and $t_{Cl} = 1/k_{Cl}[Cl]$, at room temperature, by using a spatially uniform diurnal global average for [OH] and [Cl] of 1×10^6 [64] and 1×10^4 molecule cm^{-3},[23] respectively. For several reactive HFEs, the reaction with Cl atoms contributes to more than 10% of their total tropospheric removal. Since HFCs and HFEs are widely thought to be benign to stratospheric ozone, their presence in the atmosphere is mainly associated with the problem of global warming. However, the lower tropospheric lifetimes of HFEs minimize their contribution to the greenhouse effect, suggesting that they probably constitute a more environment-friendly class of CFC substitutes than HFCs. Furthermore, the final product analysis has shown that the tropospheric degradation of HFEs results in the formation of fluorinated esters and aldehydes, COF_2, HF and CO_2.[6−9,11,13] Besides photolysis, the polar nature of esters and aldehydes suggests that wet or dry deposition is a possible removal process for these species from the atmosphere; therefore their contribution to global warming is expected to be rather small.

The results of the present study suggest that saturated HFEs containing groups such as $-OCH_2CH_3$, $-OCH_2CF_3$, and $-CH_2OCH_3$, present the highest reactivity toward OH radicals and Cl atoms, thus they constitute the most appropriate substitutes of CFCs as far as their persistence in the atmosphere is concerned. Therefore, hydrofluoroethers of the general types $R_FOCH_2CH_3$, $R_FOCH_2CF_3$, and $R_FCH_2OCH_3$ may be considered to be environment-friendly compounds while their physical properties may be tuned for certain applications by varying the chain length, branching, and the degree of fluorination of the R_F moiety.

Acknowledgment. This work was funded by the European Commission within the Environment and Climate Program (Fourth Framework Program, F-Ethers project, ENV4-CT95-0041) and the Program for Research, Technological Development and Demonstration on “Energy, Environment and Sustainable Development, 1998-2002” (Fifth Framework Program, IAFAEE project, EVK2-CT-1999-00009). It was also partially supported by the “Excellence in the Research Institutes” Program, Action 3.3.1, funded by the Greek Ministry of Development (GSRT). The assistance of the graduate students Aristotelis M. Zaras, Vassileios G. Stefanopoulos, Iosif P. Efremidis, and Dimitrios K. Papanastasiou is gratefully acknowledged.

References and Notes

(1) Zhang, Z.; Saini, R. D.; Kurylo, M. J.; Huie, R. E. *J. Phys. Chem.* **1992**, *96*, 9301−9304.

(2) Cooper, D. L.; Cunningham, T. P.; Allan, N. L.; McCulloch, A. *Atmos. Environ.* **1992**, *26A*, 1331−1334.

(3) Hsu, K.-J.; DeMore, W. B. *J. Phys. Chem.* **1995**, *99*, 11141−11146.

(4) Zang, Z.; Saini, R. D.; Kurylo, M. J.; Huie, R. E. *J. Phys. Chem.* **1992**, *96*, 9301−9304.

(5) Garland, N. L.; Medhurst, L. J.; Nelson, H. H. *J. Geophys. Res.* **1993**, *98*, 23107−23111.

(6) Wallington, T. J.; Schneider, W. F.; Sehested, J.; Bilde, M.; Platz, J.; Nielsen, O. J.; Christensen, L. K.; Molina, M. J.; Molina, L. T.; Wooldridge, P. W. *J. Phys. Chem.* **1997**, *101*, 8264−8274.

(7) Christensen, L. K.; Sehested, J.; Nielsen, O. J.; Bilde, M.; Wallington, T. J.; Guschkin, A.; Molina, L. T.; Molina, M. J. *J. Phys. Chem. A* **1998**, *102*, 4839−4845.

(8) Nolan, S.; O’Sallivan, N.; Wenger, J.; Sidebottom, H.; Treacy, J. *Proceedings of the EUROTRAC Symposium ’98, Garmisch-Partenkirchen, Germany*, 1998.

(9) Wallington, T. J.; Guschkin, A.; Stein, T. N. N.; Platz, J.; Sehested, J.; Christensen, L. K.; Nilesen, O. J. *J. Phys. Chem. A* **1998**, *102*, 1152−1161.

(10) Kambanis, K. G.; Lazarou, Y. G.; Papagiannakopoulos, P. *J. Phys. Chem. A* **1998**, *102*, 8620−8625.

(11) Christensen, L. K.; Wallington, T. J.; Guschkin, A.; Hurley, M. D. *J. Phys. Chem. A* **1999**, *103*, 4202−4208.

(12) Orkin, V. L.; Villenave, E.; Huie, R. E.; Kurylo, M. J. *J. Phys. Chem. A* **1999**, *103*, 9770−9779.

(13) Good, S. A.; Francisco, J. S. *J. Phys. Chem. A* **1999**, *103*, 5011−5014.

(14) Sekiya, A.; Misaki, S. *J. Fluorine Chem.* **2000**, *101*, 215−221.

(15) Good, S. A.; Francisco, J. S. *J. Phys. Chem. A* **1998**, *102*, 1854−1864.

(16) Good, S. A.; Francisco, J. S. *J. Phys. Chem. A* **1998**, *102*, 7143−7148.

(17) Good, S. A.; Kamboures, M.; Santiano, R.; Francisco, J. S. *J. Phys. Chem. A* **1999**, *103*, 9230−9240.

(18) Lazarou, Y. G.; Papagiannakopoulos, P. *Chem. Phys. Lett.* **1999**, *301*, 19−28.

(19) Chandra, A. K.; Uchimaru, T. *Chem. Phys. Lett.* **2001**, *334*, 200−206.

(20) DeMore, W. B.; Sander, S. P.; Golden, D. M.; Hampson, R. F.; Kurylo, M. J.; Howard, C. J.; Ravishankara, A. R.; Kolb, C. E.; Molina, M. J. *Chemical Kinetics and Photochemical Data for Use in Stratospheric, JPL Publication 97-4*, 1997.

(21) Finlayson-Pitts, B. J.; Ezell, M. J.; Pitts, J. N. J. *Nature* **1989**, *337*, 241−244.

(22) Rudolph, J.; Koppmann, R.; Plass-Dulmer, C. *Atmos. Environ.* **1996**, *30*, 1887−1894.

(23) Spicer, C. W.; Chapman, E. G.; Finlayson-Pitts, B. J.; Plastridge, R. A.; Hubbe, J. M.; Fast, J. D.; Berkowitz, C. M. *Nature* **1998**, *394*, 353−356.

(24) Vogt, R.; Crutzen, P. J.; Sander, R. *Nature* **1996**, *383*, 327−330.

(25) Tanaka, P. L.; Oldfield, S.; Neece, J. D.; Mullins, C. B.; Allen, D. T. *Environ. Sci. Technol.* **2000**, *34*, 4470−4473.

(26) Hickson, K. M.; Smith, I. W. M. *Int. J. Chem. Kinet.* **2001**, *33*, 165−172.

(27) Wallington, T. J.; Hurley, M. D.; Fedotov, V.; Morrell, C.; Hancock, G. *J. Phys. Chem. A* **2002**, *106*, 8391−8398.

(28) Nohara, K.; Toma, M.; Kutsuna, S.; Takeuchi, K.; Ibusuki, T. *Environ. Sci. Technol.* **2001**, *35*, 114−120.

(29) Ninomiya, Y.; Kawasaki, M.; Guschin, A.; Molina, L. T.; Molina, M. J.; Wallington, T. J. *Environ. Sci. Technol.* **2000**, *34*, 2973−2978.

(30) Mashino, M.; Kawasaki, M.; Wallington, T. J.; Hurley, M. D. *J. Phys. Chem. A* **2000**, *104*, 2925−2930.

(31) Lazarou, Y. G.; Michael, C.; Papagiannakopoulos, P. *J. Phys. Chem.* **1992**, *96*, 1705−1708.

(32) Lazarou, Y. G.; Prosmitis, A. V.; Papadimitriou, V. C.; Papagiannakopoulos, P. *J. Phys. Chem. A* **2001**, *105*, 6729−6742.

(33) Zhan, C.-G.; Nichols, J. A.; Dixon, D. A. *J. Phys. Chem. A* **2003**, *107*, 4184−4195.

(34) Kambanis, K. G.; Lazarou, Y. G.; Papagiannakopoulos, P. *Int. J. Chem. Kinet.* **1995**, *27*, 343−349.

(35) Frisch, M. J.; Trucks, G. W.; Schlegel, H. B.; Scuseria, G. E.; Robb, M. A.; Cheeseman, J. R.; Zakrzewski, V. G.; Montgomery, J. A., Jr.; Stratmann, R. E.; Burant, J. C.; Dapprich, S.; Millam, J. M.; Daniels, A. D.; Kudin, K. N.; Strain, M. C.; Farkas, O.; Tomasi, J.; Barone, V.; Cossi, M.; Cammi, R.; Mennucci, B.; Pomelli, C.; Adamo, C.; Clifford, S.; Ochterski, J.; Petersson, G. A.; Ayala, P. Y.; Cui, Q.; Morokuma, K.; Malick, D. K.; Rabuck, A. D.; Raghavachari, K.; Foresman, J. B.; Cioslowski, J.; Ortiz, J. V.; Baboul, A. G.; Stefanov, B. B.; Liu, G.; Liashenko, A.; Piskorz, P.; Komaromi, I.; Gomperts, R.; Martin, R. L.; Fox, D. J.; Keith, T.; Al-Laham, M. A.; Peng, C. Y.; Nanayakkara, A.; Gonzalez, C.; Challacombe, M.; Gill, P. M. W.; Johnson, B.; Chen, W.; Wong, M. W.; Andres, J. L.; Gonzalez, C.; Head-Gordon, M.; Replogle, E. S.; Pople, J. A. *Gaussian 98*, Revision A.7; Gaussian, Inc., Pittsburgh, PA, 1998.

(36) Becke, A. D. *J. Chem. Phys.* **1993**, *98*, 5648.

(37) Perdew, J. P. *Phys. Rev. B* **1986**, *33*, 8822.

(38) Petersson, G. A.; Al-Laham, M. A. *J. Chem. Phys.* **1991**, *94*, 6081.

(39) Binning, R. C. J.; Curtiss, L. A. *J. Comput. Chem.* **1990**, *11*, 1206.

(40) McLean, A. D.; Chandler, G. S. *J. Chem. Phys.* **1980**, *72*, 5639.

(41) Pilcher, G.; Pell, A. S.; Coleman, D. J. *Trans. Faraday Soc.* **1964**, *60*, 499−505.

(42) Benson, S. W. *Thermochemical Kinetics*, 2nd ed.; Wiley-Interscience, New York, 1976.

(43) Cox, J. D.; Wagman, D. D.; Medvedev, V. A. *CODATA Key Values for Thermodynamics*; Hemisphere Publishing Corp.: New York, 1984.

(44) Butler, J. J.; Holland, D. M. P.; Parr, A. C.; Stockbauer, R. *Int. J. Mass Spectrom. Ion Processes* **1984**, *58*, 1.

(45) Bowen, R. D.; Maccoll, A. *Org. Mass Spectrom.* **1984**, *19*, 379.

(46) Molder, U. H.; Pikver, R. J.; Koppel, I. A. *Org. React. (N. Y. Engl. Transl.)* **1983**, *20*, 208.

(47) Evans, M. G.; Polanyi, M. *Trans. Faraday Soc.* **1938**, *34*, 11.

(48) Donahue, N. M.; Clarke, J. S.; Anderson, J. G. *J. Phys. Chem. A* **1998**, *102*, 3923−3933.

(49) Donahue, N. M. *J. Phys. Chem. A* **2001**, *105*, 1489−1497.

(50) Bartolotti, L. J.; Edney, E. O. *Int. J. Chem. Kinet.* **1994**, *26*, 913−920.

(51) Atkinson, R. *Chem. Rev.* **1985**, *85*, 69−201.

(52) Kwok, E. S. C.; Atkinson, R. *Atmos. Environ.* **1995**, *29*, 1685−1695.

(53) Cohen, N.; Benson, S. W. *J. Phys. Chem.* **1987**, *91*, 171−175.

(54) Chiorboli, C.; Piazza, R.; Tosato, M. L.; Carassiti, V. *Coord. Chem. Rev.* **1993**, *1993*, 241−250.

(55) Klamt, A. *Chemosphere* **1993**, *26*, 1273−1289.

(56) Michael, J. V.; Nava, D. F.; Payne, W. A.; Stief, L. J. *J. Phys. Chem.* **1979**, *70*, 3652−3656.

(57) Wine, P. H.; Semmes, D. H. *J. Phys. Chem.* **1983**, *87*, 3572−3578.

(58) Tschuikow-Roux, E.; Yano, T.; Niedzelski, J. *J. Phys. Chem.* **1984**, *88*, 1408−1414.

(59) Tschuikow-Roux, E.; Niedzelski, J.; Faraji, F. *Can. J. Chem.* **1985.**, *63*, 1093−1099.

(60) Senkan, S. M.; Quam, D. *J. Phys. Chem.* **1992**, *96*, 10837−10842.

(61) McLoughlin, P.; Kane, R.; Shanahan, I. *Int. J. Chem. Kinet.* **1993**, *25*, 137−149.

(62) Miyokawa, K.; Tschuikow-Roux, E. *J. Phys. Chem.* **1990**, *94*, 715−717.

(63) Lazarou, Y. G.; Papadimitriou, V. C.; Prosmitis, A. V.; Papagiannakopoulos, P. *J. Phys. Chem. A* **2002**, *106*, 11502−11517.

(64) Kley, D. *Science* **1997**, *276*, 1043−1045.

(65) Chen, L.; Kutsuna, S.; Nohara, K.; Takeuchi, K.; Ibusuki, T. *J. Phys. Chem. A* **2001**, *105*, 10854−10859.

(66) Heathfield, A. E.; Anastasi, C.; Pagsberg, P.; McCulloch, A. *Atmos. Environ.* **1998**, *32*, 711−717.

(67) Tokuhashi, K.; Takahashi, A.; Kaise, M.; Kondo, S.; Sekiya, A.; Yamashita, S.; Ito, H. *J. Phys. Chem. A* **2000**, *104*, 1165−1170.

(68) Tokuhashi, K.; Takahashi, A.; Kaise, M.; Kondo, S.; Sekiya, A.; Yamashita, S.; Ito, H. *Int. J. Chem. Kinet.* **1999**, *31*, 846−853.

(69) Chen, L.; Kutsuna, S.; Tokuhashi, K.; Sekiya, A.; Takeuchi, K.; Ibusuki, T. *Int. J. Chem. Kinet.* **2003**, *35*, 239−245.

(70) Tokuhashi, K.; Takahashi, A.; Kaise, M.; Kondo, S. *J. Geophys. Res.* **1999**, *D15*, 18681.

(71) Brown, A. C.; Canosa-Mas, C. E.; Parr, A. D.; Wayne, R. P. *Atmos. Environ.* **1990**, *24A*, 2499−2511.

(72) Tokuhashi, K.; Takahashi, A.; Kaise, M.; Kondo, S.; Sekiya, A.; Fujimoto, E. *Chem. Phys. Lett.* **2000**, *325*, 189−195.

(73) Chen, J.; Young, V.; Niki, H.; Magid, H. *J. Phys. Chem. A* **1997**, *101*, 2648−2653.

(74) Barry, J.; Locke, G.; Scollard, D.; Sidebottom, H. T., J.; Clerbaux, C.; Colin, R.; Franklin, J. *Int. J. Chem. Kinet.* **1997**, *29*, 607−617.

(75) Mogelberg, T. E.; Sehested, J.; Bilde, M.; Wallington, T. J.; Nielsen, O. J. *J. Phys. Chem.* **1996**, *100*, 8882−8889.